

High-resolution neutron powder diffraction study on the phase transitions in BaPbO₃

W.T. Fu^{a,*}, D. Visser^b, K.S. Knight^c, D.J.W. IJdo^a

^aLeiden Institute of Chemistry, Gorlaeus Laboratories, Leiden University, P.O. Box 9502, 2300 RA Leiden, The Netherlands

^bNWO-Physics, ISIS Facility, Rutherford Appleton Laboratory, Chilton, Didcot OX11 0QX, UK

^cISIS Facility, Rutherford Appleton Laboratory, Chilton, Didcot OX11 0QX, UK

Received 9 November 2006; received in revised form 10 February 2007; accepted 2 March 2007

Available online 12 March 2007

Abstract

Phase transitions that occurred in perovskite BaPbO₃ have been investigated using high-resolution time-of-flight neutron powder diffraction. The structure at room temperature is orthorhombic (space group *Imma*), which is derived from the cubic aristotype by tilting the PbO₆ octahedra around the two-fold axis (tilt system $a^0b^-b^-$). The orthorhombic structure shows anisotropic line broadening attributed to the presence of micro twins. At above about 573 K, BaPbO₃ undergoes a discontinuous phase transition to a tetragonal structure (space group *I4/mcm*) with the tilting of the PbO₆ octahedra being about the four-fold axis of the cubic aristotype (tilt system $a^0a^0c^-$). With further increasing the temperature, BaPbO₃ experiences a continuous phase transition to a simple cubic structure (space group *Pm $\bar{3}m$*) at above about 673 K. The later phase transition is characterised by a critical exponent of $\beta = 0.36$, depicted by the three-dimensional Heisenberg universality class. The earlier reported *Imma* → *I2/m* phase transition above room temperature has not been observed.

© 2007 Elsevier Inc. All rights reserved.

Keywords: Perovskites; High-resolution neutron powder diffraction; Crystal structure; Phase transition

1. Introduction

Temperature induced phase transitions in the perovskite family have received renewed attention in recent years with much interest in what should be the logical phase sequence as well as the nature of the phase transitions. The ideal perovskite of the formula *ABO*₃ has a simple cubic structure and belongs to the space group *Pm $\bar{3}m$* . This structure generally requires the Goldsmith tolerance factor, $t = (r_A + r_O) / \sqrt{2}(r_B + r_O)$, to be very close to unity ($t \approx 1$). The majority of the perovskites do not, however, fulfil this condition and their structures at room temperature or below distort from the cubic symmetry. Based on the tolerance factor, the distortion mechanisms are usually described as *A*-cation driven ($t < 1$) or *B*-cation driven ($t > 1$). In the first case, the cuboctahedral cavity formed by

corner-linked *BO*₆ octahedra is too large for *A*, and, consequently, the *BO*₆ octahedra tilt cooperatively to reduce the size of the cavity. On the contrary, when $t > 1$, the *B*-cation is nominally too small for its octahedral site, and may tend to displace. Between the two distortion mechanisms, the *A*-cation driven is most common. In particular, since the *BO*₆ octahedra have many tilting possibilities, this type of distortion results also in many different structures. Glazer [1,2] analysed the different tilting patterns in terms of component tilts around three axes of the cubic aristotype, and obtained 23 tilt systems. Although the Glazer's classification of the tilt systems may be very helpful in analysing the structure of the tilt perovskites, it provides no information on what would be the logical phase sequence if a perovskite undergoes phase transitions, when the external conditions, e.g. temperature and pressure, change. Recently, Howard and Stokes [3] have, using group theoretical methods, re-analysed the problem of the octahedral tilting in simple perovskites.

*Corresponding author. Fax: +31 71 5274537.

E-mail address: w.fu@chem.leidenuniv.nl (W.T. Fu).

They listed 15 possible space groups for all tilt systems. They also presented a diagram displaying the group–subgroup relationships and the nature of the corresponding phase transitions, i.e. being either discontinuous or possibly continuous.

The continuous phase transitions are traditionally analysed in terms of the Landau free energy expansion containing even-order terms [4]:

$$G = \frac{1}{2}a(T - T_c)Q^2 + \frac{1}{4}BQ^4 + \frac{1}{6}cQ^6 + \dots, \quad (1)$$

where Q is the order parameter; T_c is the critical temperature and A , B , C etc are coefficients. Two cases that the Landau expansion describes continuous phase transition are:

- (i) When B is positive and the sixth-order term is negligibly small, the expansion depicts a second-order phase transition. Minimising Eq. (1) ($\partial G/\partial Q = 0$) gives

$$Q = \left[\frac{a}{B}(T - T_c) \right]^{1/2}. \quad (2)$$

- (ii) When $B = 0$, the Landau expansion must include the six-order term with c positive to produce a minimum in the low temperature form. This case, being called ‘tricritical’, gives the equilibrium variation of Q with temperature as

$$Q = \frac{a}{c}(T - T_c)^{1/4}. \quad (3)$$

Eqs. (2) and (3) can be written in a more generalised form:

$$Q = A(T - T_c)^\beta, \quad (4)$$

where β is termed the critical exponent and describes the variation of the order parameter with temperature for continuous transitions. For the two ideal cases considered above, $\beta = 0.5$ and 0.25 for a second order and a tricritical transition, respectively.

In the past years, the temperature dependent phase transitions of a number of $A(\text{II})B(\text{IV})\text{O}_3$ -type perovskites have been studied, and several transition pathways were reported. For example, in SrZrO_3 [5,6], SrHfO_3 [7], SrRuO_3 [8,9] and BaTbO_3 [10], the phase sequence, by increasing temperature, is $Pnma \rightarrow Imma \rightarrow I4/mcm \rightarrow Pm\bar{3}m$, thought the $Pnma$ structure does not occur in BaTbO_3 . In BaCeO_3 [11], the observed phase sequence is $Pnma \rightarrow Imma \rightarrow R\bar{3}c \rightarrow Pm\bar{3}m$. In addition, the $I4/mcm \rightarrow Pm\bar{3}m$ phase transition was reported to be characteristic of a continuous transition, but the critical exponents are rather divergent, e.g. $\beta = 0.25$ in SrZrO_3 [6], $\beta = 0.5$ in SrHfO_3 [7] and $\beta = 0.35$ in BaTbO_3 [10].

For BaPbO_3 , another phase sequence, $Pm\bar{3}m \rightarrow I4/mcm \rightarrow Imma \rightarrow I2/m$, has been reported, which is yet poorly characterised. Ivanov et al. [12] have, from neutron powder diffraction data, studied the structures of BaPbO_3 between 300 and 1000 K with rough temperature steps.

They listed the following structures: $I2/m$ ($T = 300$ K), $Imma$ ($T = 500$ K), $I4/m$ ($T = 600$ K) and $Pm\bar{3}m$ ($T = 800$ K). In their published work, however, neither the transition temperatures nor the detailed analyses that may prove the assigned space groups were given. Moussa et al. [13] have investigated the structures of BaPbO_3 below room temperature using neutron powder diffraction in combination with synchrotron X-ray diffraction. They concluded that the space group of BaPbO_3 is $Imma$ at room temperature and transforms to $I2/m$ at low temperature (e.g. at $T = 15$ K). They also suggested the $Imma \rightarrow I2/m$ transition below room temperature being continuous; but the transition temperature was, again, not determined. Hester et al. [14] have studied the structures of BaPbO_3 above room temperature using high-resolution X-ray synchrotron diffraction, and found the following successive phase transitions: $Imma \rightarrow I4/mcm \rightarrow Pm\bar{3}m$, occurring at above about 613 and 763 K, respectively. The $I4/mcm \rightarrow Pm\bar{3}m$ phase transition was ascribed to be continuous having tricritical characteristic. Although the authors have also carried out the structural refinements, the data were not directly given in their publication.

Clearly, the important difference between the reported phase sequence in BaPbO_3 and those in other known $A(\text{II})B(\text{IV})\text{O}_3$ -type perovskites [5–11] is the occurrence of the $I2/m$ structure. Although, $I2/m$ is a subgroup of $Imma$ [3] and the $Imma \rightarrow I2/m$ phase transition might be expected as logical, the correctness of assigning the $I2/m$ structure for BaPbO_3 at either above [12] or below room temperature [13] is questionable. For example, the tilt system ($a^0b^-c^-$) ($I2/m$) is, actually, the intermediate between the tilt system ($a^0b^-b^-$) ($Imma$) and the tilt system ($a^0b^0c^-$) ($I4/mcm$), in which two tilting angles are equal and at least one tilting angle is zero. As such tilt system results in a twisted basal plane, whether this geometry of octahedron would be adopted by a tilt perovskite is unclear. In fact, many perovskites show the $Imma \rightarrow Pnma$ phase transition, when larger tilting angle is required. Recently, we carried out a high-resolution time-of-flight powder neutron diffraction study on the structure of BaPbO_3 between room temperature and 4.2 K [15]. By analyzing the FWHM-values of the observed reflection profiles, we found that the line broadening that occurs in BaPbO_3 is not due to the monoclinic distortion as was previously suggested [12,13,16], but has the anisotropic nature attributable to the presence of micro twins that introduces strains along the orthorhombic [110]-axis. The structure of BaPbO_3 at room temperature and 4.2 K is thus modelled in the orthorhombic $Imma$ space group by introducing anisotropic line broadening [15].

In the present investigation, the phase transitions in BaPbO_3 at high temperature have further been studied by high-resolution time-of-flight powder neutron diffraction. Since this technique provides high enough resolution combined with high sensitivity of neutron to oxygen scattering, it is particularly suitable for revealing structural changes and for studying the nature of the phase transitions in tilt perovskites. Our results confirmed

BaPbO₃ transforming from the orthorhombic *Imma* structure to the cubic *Pm $\bar{3}m$* through the intermediate tetragonal *I4/mcm* phase [12,14], but the transition temperatures were found to be significantly lower (at about 565 and 660 K, respectively) than those determined from the X-ray synchrotron diffraction data (~ 673 and ~ 763 K, respectively) [14]. In addition, the continuous *I4/mcm* \rightarrow *Pm $\bar{3}m$* phase transition is neither a mean field second order nor is a tricritical transition; the tilting angle as the function of temperature shows the critical exponent characteristic of the Heisenberg universality class instead. We report the results in this paper.

2. Experimental

Samples for neutron powder diffraction were prepared from the BaCO₃ and PbO powders in alumina crucible. The stoichiometric mixture was intimately ground in ethanol. After drying, the mixtures were first reacted at 800 °C over night to avoid possible loss of lead oxide. The resultant powder was then sintered at 850, 900 and 950 °C, respectively, with 20 h at each temperature step accompanied by intermittent regrinding. The sample was, finally, slowly cooled to room temperature in about 15 h. All sintering and cooling were carried out in oxygen flow.

X-ray powder diffraction was carried out to check the sample's purity using a Philips PW1050 diffractometer using monochromatic CuK α radiation. High-resolution time-of-flight powder neutron diffraction data were collected with the HRPD diffractometer at the ISIS Facility, Rutherford Appleton Laboratories. The sample was loaded into a 11 mm diameter vanadium can and mounted in a furnace. The measurements were performed on heating at each temperature step (20 °C). The diffraction patterns were recorded in both the backscattering bank and the 90°-detector bank, over the time-of-flight range 32–120 ms and 35–114 ms, corresponding to the *d*-spacings from 0.6 to 2.5 Å and 1.0 to 3.3 Å respectively. The patterns were normalized to the incident beam spectrum as recorded in the upstream monitor, and corrected for detector efficiency according to prior calibration with vanadium (rod). Most patterns were recorded to a total incident proton beam of about 35 μ Ah, in approximately 2 h. Calculations were performed simultaneously on both backscattering and 90°-bank data by the Rietveld method using the GSAS computer programme [17].

3. Results

The structural changes in BaPbO₃ as the function of temperature can easily be seen by inspecting the splitting of the (200) and (222) reflections of the cubic aristotype shown in Fig. 1. Between room temperature and below about 573 K, both the (200) and (222) reflections split in a doublet, which are characteristic of an orthorhombic distortion. In this temperature range, it is also observed that the (*hkl*) reflections show the systematic line broad-

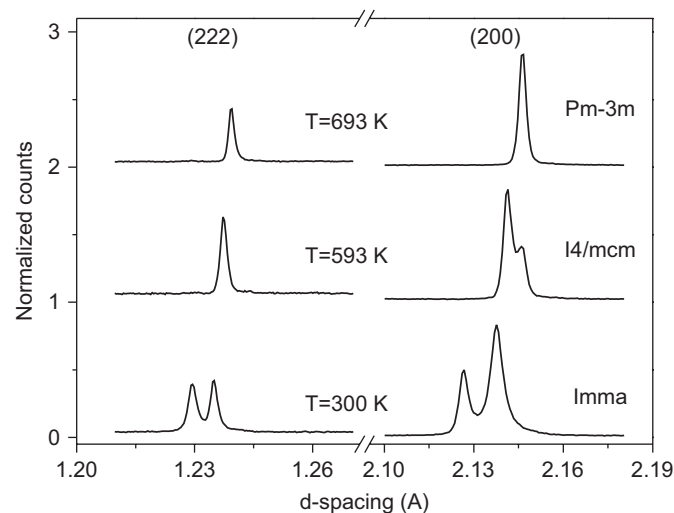


Fig. 1. A section of the high-resolution backscattering neutron diffraction pattern showing the evolution of the (200) and (222) reflections of the cubic aristotype in BaPbO₃ at some representative temperatures. The significance of the peak splitting, broadening and the change of their relative intensities are discussed in the text. Note that the intensity of the (222) reflection has been multiplied by 3 for visualisation purpose.

ening as compared to that of the (00*l*) reflections. An example is shown in Fig. 1: the peak at longer *d*-spacing side of the (200) doublet (indexed as (220) in an orthorhombic cell of the dimension $a \approx b \approx \sqrt{2}a_p$ and $c \approx 2a_p$) is markedly broader than that at shorter *d*-spacing side (indexed as (004)) (Fig. 1). Although such line broadenings have previously been described as due to the monoclinic distortion [13,16], the same kind of broadenings exists, in fact, in the whole orthorhombic phase region, disproving the possibility of the *I2/m* \rightarrow *Imma* phase transition above room temperature. As was shown by the recent high-resolution neutron powder diffraction study [15], the anisotropic line broadening in BaPbO₃ is likely due to the presence of micro twins that introduce strains along the orthorhombic [110]-direction. Therefore, the structure of BaPbO₃ at 300 K \leq *T* < 573 K is modelled in the space group *Imma* by adding the refinable γ coefficients in the profile function that accounts for the strain induced anisotropic line broadening.

At the temperature of about above 573 K, the doublet of the (222) reflection disappears and that of the (200) reflection remains with the reversed intensity ratio (Fig. 1). This is typically of a tetragonal distortion, indicating a change of the tilting direction of the octahedra from the [110]-axis to the [001]-axis of the cubic aristotype. The structure of BaPbO₃ is described in the space group *I4/mcm* as was reported earlier [12,14]. As the temperature increases to above about 633 K, the splitting of the (200) reflection becomes non-resolvable within the instrument resolution, but the tetragonal structure persists as indicated by the presence of the superstructure reflections. The neutron powder diffraction patterns at above about 673 K do not show any trace of the superstructure reflections, suggesting that the structure of BaPbO₃ becomes primitive

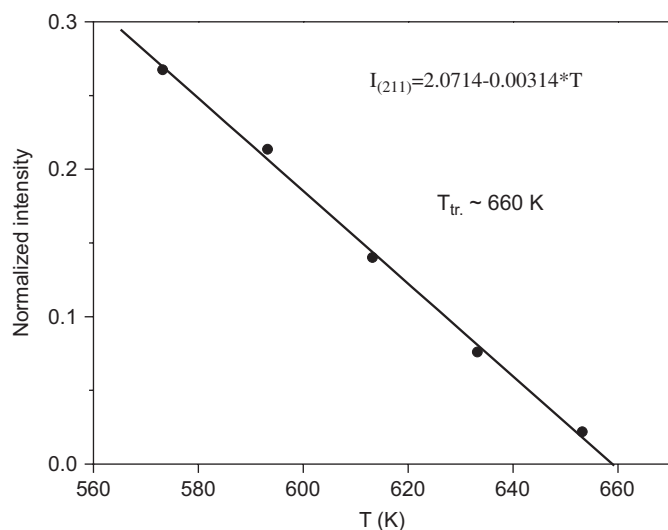


Fig. 2. Variation of the normalised neutron diffraction intensity of the tetragonal (211) superstructure reflection as the function of temperature. Insert gives linear fitting with the extrapolated transition temperature of 660 K.

cubic. To estimate the transition temperature, we plotted in Fig. 2 the normalised intensity of the tetragonal (211) reflection (revealed in our 90°-bank data) as the function of temperature, and found it to decrease quite linearly with increasing temperature. From the linear extrapolation, a transition temperature at about 660 K is expected, which is in good agreement with the experimentally observed value (see also discussion below).

The structural refinements were, therefore, carried out in the space groups $Imma$,¹ $I4/mcm$ and $Pm\bar{3}m$, respectively. All refinements yielded satisfactory results. Table 1 summarizes the refined lattice parameters and atomic positions of BaPbO₃ in three different phases. Fig. 3 shows the plots of the observed and calculated profiles at some representative temperatures. Some selected interatomic distances are listed in Table 2.

4. Discussion

Below about 573 K, BaPbO₃ crystallises in the orthorhombic space group $Ibmm$, in which the PbO₆ octahedra tilted around the [110]-axis of the cubic aristotype. The tilting angle decreases smoothly between 300 and 573 K ranging from 8.6° to 5.8° (Fig. 4). In this temperature range, the a -axis remains virtually constant whereas the b - and c -axis gradually expand (Fig. 5). The same behaviour has been seen in BaTbO₃ in the same structure region and is expected by the fact that the tilting angle is about the orthorhombic a -axis.

When the temperature is raised to above about 573 K, the structure of BaPbO₃ changes to tetragonal with the

space group $I4/mcm$, characterised by the reduced cell parameter ratio $c_r/a_r > 1$. Since this structural transformation involves the changing of tilting directions of the PbO₆ octahedra, i.e. from around the two-fold axis to the four-fold axis, the $Imma \rightarrow I4/mcm$ transition must be a first-order phase transition [3]. Although the change of the lattice parameters across the $Imma \rightarrow I4/mcm$ phase transition do not apparently show abrupt discontinuity (Fig. 5a), the variation of the reduced cell volume exhibits a kind of discontinuousness (Fig. 5b). This behaviour has also been observed in BaTbO₃ [10], though the later compound shows somewhat larger step-like change in the cell volume across of the same phase transition.

In BaPbO₃, the tetragonal $I4/mcm$ structure exists in a relatively narrow temperature range of roughly 100 K. The tilting angle in this temperature range decreases smoothly with increasing the temperature (Fig. 4) and the variation of the lattice parameters/cell volume across the phase transition shows no obvious discontinuity (Fig. 5). As the $I4/mcm \rightarrow Pm\bar{3}m$ is known to be continuous, we have evaluated the critical exponent as well as the transition temperature using the generalised Eq. (4). We chose the tilting angle (φ) as the order parameter and fitted its variation with the temperature. The experimentally fitted values are: $T_c = 658(1)$ K, $\beta = 0.36(2)$ with $A = 1.1(1)$. The obtained T_c -value is in good agreement with the experimental results that show the transition temperature lying between 653 and 673 K. The β -value is, however, not the one expected from the classic Landau theory either for a mean-field second-order transition ($\beta = 0.5$) or for a tricritical transition ($\beta = 0.25$) [4]. On the other hand, a similar behaviour has previously been observed in BaTbO₃ ($\beta = 0.35$) [10]. Also a comparable value ($\beta = 0.37$) has been seen in SrRuO₃ for the same phase transition [18]. Coincidentally, in the perovskites CeAlO₃ and LaAlO₃ [19], the analogous values, $\beta = 0.35$ and 0.36 respectively, exist as well for the continuous $R\bar{3}c \rightarrow Pm\bar{3}m$ phase transition.

It is interesting to consider whether the continuous phase transitions in perovskites may share some common feature. The continuous phase transitions are characterized by the critical phenomena associated with the critical points. In the critical region, some physically measurable parameters, known as the order parameters, follow typically power law behaviour with the characteristic critical exponent (β). As was mentioned above, the Landau approach yields the critical exponent $\beta = 0.5$ for second-order phase transition (4). In case that the coefficient of the fourth power of the order parameter in the Landau free energy expansion is negligible, a case termed as tricritical, the critical exponent of $\beta = 0.25$ is expected. Among the recently studied phase transitions in the ABO₃-type perovskites, both exponents have been reported; the tilting angle as the function of temperature was found to have the critical exponent of 0.5 in SrHfO₃ [7] and 0.25 for the structurally related SrZrO₃ [5,6]. However, it is known that the Landau theory predicts the incorrect critical exponents for the continuous

¹For easy comparison with the tetragonal structure, the space group $Ibmm$, instead of the standard $Imma$, was used with the c -axis as the longest one.

Table 1
Refined atomic positions and thermal parameters of BaPbO₃ at some selected temperatures

<i>T</i> (K)	373	473	553	573	613	633	673	773
Space group	<i>Ibmm</i>	<i>Ibmm</i>	<i>Ibmm</i>	<i>I4/mcm</i>	<i>I4/mcm</i>	<i>I4/mcm</i>	<i>Pm</i> $\bar{3}$ <i>m</i>	<i>Pm</i> $\bar{3}$ <i>m</i>
<i>a</i> (Å)	6.06607(5)	6.06713(6)	6.06601(8)	6.05221(3)	6.05917(3)	6.06325(4)	4.29202(1)	4.29970(1)
<i>b</i> (Å)	6.03375(5)	6.04436(6)	6.05299(7)					
<i>c</i> (Å)	8.52065(6)	8.53976(6)	8.55447(7)	8.57946(8)	8.58281(7)	8.58215(10)		
Pb	4 <i>a</i> (0, 0, 0)			4 <i>c</i> (0, 0, 0)			1 <i>a</i> (0, 0, 0)	
<i>B</i> (Å ²)	1.06(2)	1.21(2)	1.30(2)	1.38(3)	1.41(2)	1.46(3)	1.55(3)	1.68(3)
Ba	4 <i>e</i> (<i>x</i> , 0, 1/4)			4 <i>b</i> (1/2, 0, 1/4)			1 <i>b</i> (1/2, 1/2, 1/2)	
	<i>x</i> : 0.4996(4)	0.4989(6)	0.4983(11)					
<i>B</i> (Å ²)	1.44(3)	1.81(3)	2.01(4)	2.13(4)	2.16(4)	2.35(4)	2.50(4)	2.81(4)
O(1)	4 <i>e</i> (<i>x</i> , 0, 1/4)			4 <i>a</i> (0, 0, 1/4)			3 <i>d</i> (1/2, 0, 0)	
	<i>x</i> : 0.0455(3)	0.0396(4)	0.0313(6)					
<i>B</i> (Å ²)	2.45(6)	2.81(8)	3.01(11)	3.97(11)	4.15(11)	4.83(23)	4.84(4)	5.12(4)
O(2)	8 <i>g</i> (1/4, 1/4, <i>z</i>)			8 <i>h</i> (<i>x</i> , 1/2 + <i>x</i> , 0)				
	<i>z</i> : −0.0252(1)	−0.0223(2)	−0.0192(3)	<i>x</i> : 0.2732(2)	0.2687(2)	0.2648(2)		
<i>B</i> (Å ²)	2.64(4)	3.37(5)	4.07(7)	3.87(6)	4.05(6)	4.21(10)		
<i>R</i> _{wp} (%)	6.08	6.27	6.62	7.01	6.87	7.07	7.40	7.30
<i>R</i> _p (%)	5.67	5.56	5.69	6.09	5.63	5.73	5.84	5.82

second-order phase transitions such as the Ising and liquid–gas systems. The extension of Landau theory to include the fluctuation in the order parameters, e.g. the renormalization group theory, has shown that Landau theory is only valid near the critical points of systems with spatial dimensions of 4 or higher [20]. It is also a remarkable fact that phase transitions arising in different systems often possess the same set of critical exponents. This phenomenon is known as universality. Universality is a prediction of the renormalization group theory of phase transitions, which states that the thermodynamic properties of a system near a phase transition depend only on a small number of features, such as the space dimensionality, the range of the interaction and the symmetry of the order parameter, and is insensitive to the underlying microscopic properties of the system. For instance, the critical exponents at the liquid–gas critical point have been found to be independent of the chemical composition of the fluid. More amazingly, they are an exact match for the critical exponents of the ferromagnetic phase transition. As was mentioned above, the values of the static critical exponents in several well-studied perovskites remarkably coincide despite the involved phase transitions being different. In addition, the range of validity of the critical behaviour is not confined only to the region near the critical point but extends the whole *I4/mcm* and *R* $\bar{3}$ *c* phase regions. Given that the observed critical exponents are very close to that of the three-dimensional Heisenberg universality class ($\beta = 0.3689(3)$) [21], the question arises on whether the continuous phase transitions in tilt perovskites belong to the same universality class. As a matter of fact, the notion of universality in the structural phase transitions in perovskites has been invoked long time ago by Müller

and Berlinger [22]. In their electron paramagnetic resonance (EPR) experiment on the structural phase transitions occurred in LaAlO₃ and SrTiO₃, i.e. *R* $\bar{3}$ *c* → *Pm* $\bar{3}$ *m* and *I4/mcm* → *Pm* $\bar{3}$ *m* respectively, they provided the first unambiguous evidence of deviations from the classical predictions for the static critical behaviour at the structural phase transitions. They also established a value for the order parameter exponent of $\beta = 0.33 \pm 0.02$ for these systems. The present investigation, together with those carried out for other perovskites [10,18,19], is in agreement with the earlier finding of Müller and Berlinger, being suggestive of the validity of the universality notion for continuous phase transitions in tilt perovskites. On the other hand, as the Landau-like exponent has also been reported, e.g. in SrHfO₃ [7], more experiments with high-precision are necessary to further justify the notion of the universality for this type of continuous phase transitions.

It is worth mentioning that the transition temperatures determined from high-resolution neutron powder diffraction of the present investigation are significantly lower, ~90 K, than those reported earlier [14]. The reason for such large discrepancies is unclear but could be due to the techniques that were used. While X-ray synchrotron diffraction may provide high instrument resolution, it is generally insensitive to oxygen atoms in the presence of heavy elements. In the case of BaPbO₃ with the tetragonal structure, the intensity of the strongest superstructure reflection, i.e. the (211) reflection, is only 0.08% of that of the strongest main reflections when assuming the *x*-coordinate of O₂ to be 0.2732 (see Table 1). This value decreases to less than 0.009% as the *x*-coordinate becomes 0.2573, a refined value corresponding to *T* = 653 K (not

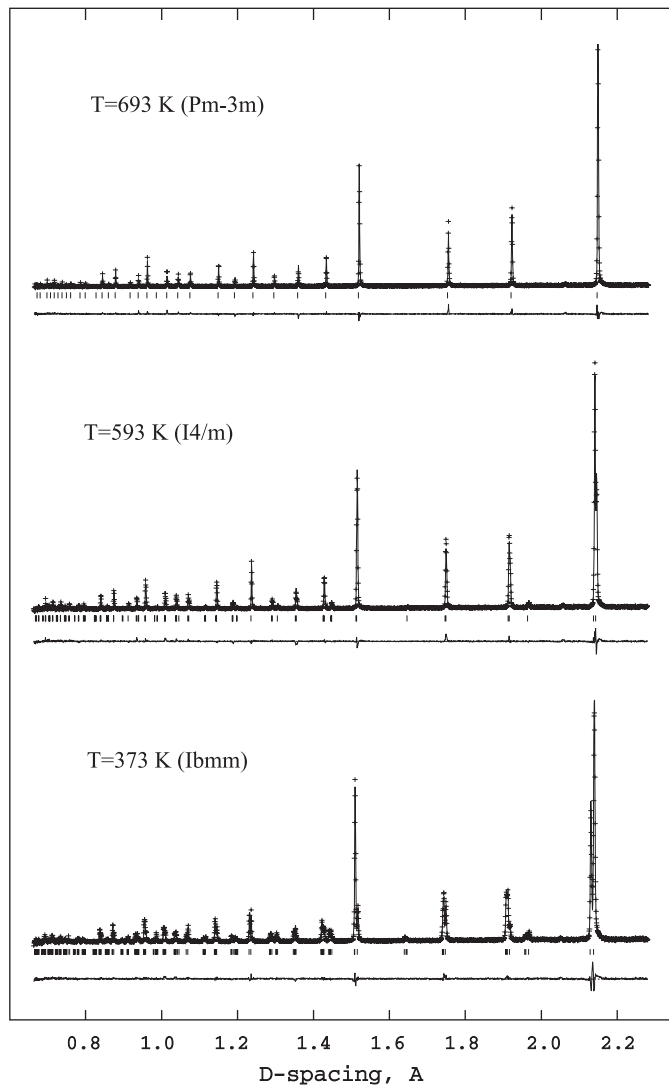


Fig. 3. Observed (crosses) and calculated (continuous line) profiles (backscattering bank data) of BaPbO_3 at $T = 300, 593$ and 693 K in the space groups $Ibmm$, $I4/m$ and $Pm\bar{3}m$ respectively. Tick marks indicate the positions of allowed reflections by each space group. The difference curve ($I_{\text{obs}} - I_{\text{cal}}$) is shown at the bottom.

Table 2
Selected interatomic distances (\AA) in BaPbO_3

T (K)	473		613		673	
Space group	$Ibmm$		$I4/m$		$Pm\bar{3}m$	
Pb–O(1)	2.1484(3)	2 ×	2.14570(1)	2 ×	2.14601(1)	6 ×
Pb–O(2)	2.1495(1)	4 ×	2.1482(1)	4 ×		
Ba–O(1)	2.787(2)		3.02958(1)	4 ×	3.03491(1)	12 ×
	3.0312(4)	2 ×				
	3.281(4)					
Ba–O(2)	2.896(2)	4 ×	2.921(1)	4 ×		
	3.158(2)	4 ×	3.147(1)	4 ×		

listed in Table 1). Such extremely weak intensity is not likely to be detected by the X-ray diffraction technique. Consequently, the neutron powder diffraction may take

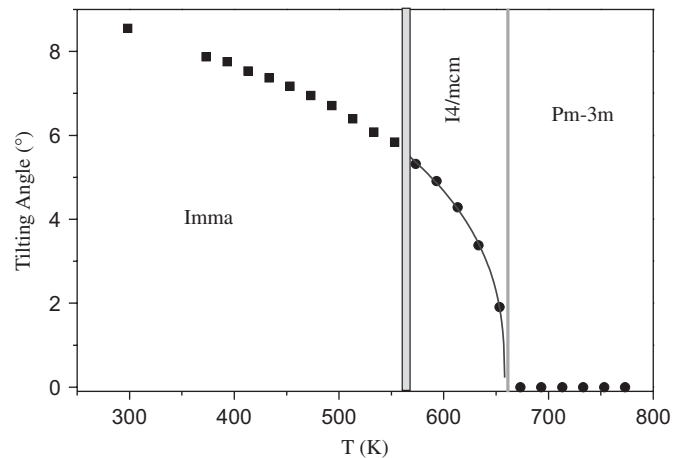


Fig. 4. Temperature dependence of the octahedral tilting angles in BaPbO_3 . The continuous line in tetragonal phase region is the fit to the expression: $\varphi = A(T_c - T)^\beta$ with the fitted values of $T_c = 658(1)$ K, $\beta = 0.36(2)$ and $A = 1.1(1)$. The shaded area indicates the possible two-phase region.

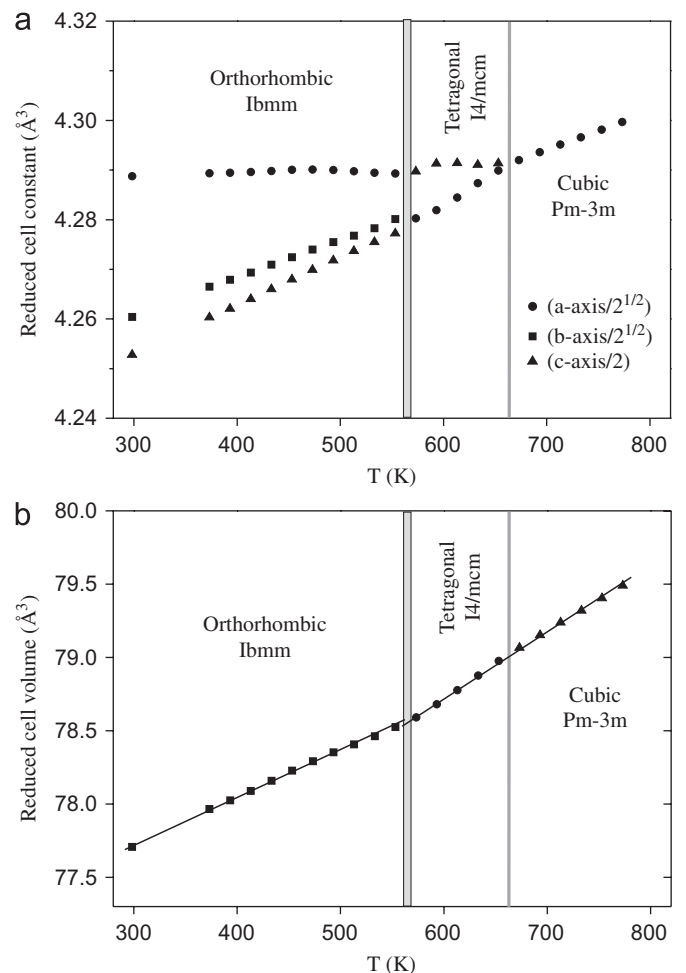


Fig. 5. Temperature dependence of (a) reduced cell constants and (b) reduced cell volume for BaPbO_3 . Note that the cell volume shows discontinuous behaviour across the $Ibmm \rightarrow I4/m$ phase transition.

advantage of revealing the positions of oxygen in the existence of heavy atoms.

In summary, the structures of BaPbO₃ at high temperature were investigated by using high-resolution time-of-flight neutron powder diffraction technique. At room temperature or below, BaPbO₃ is orthorhombic with the space group *Imma* [15]. Above room temperature, it undergoes two-phase transitions: first to the tetragonal *I4/mcm* structure and then to the primitive cubic structure, at the temperatures above about 573 and 673 K respectively. The phase sequence, *Ibmm* → *I4/mcm* → *Pm $\bar{3}$ m*, in BaPbO₃ is the one usually occurred in the distorted perovskites due to the tilting of octahedra. Once and again, the *I4/mcm* → *Pm $\bar{3}$ m* phase transition is continuous with the critical exponent of the tilting angle being characteristic of the Heisenberg universality class.

Acknowledgments

This research project has been supported by the European Commission under the 6th Framework Programme through the Key Action: Strengthening the European Research Area, Research Infrastructures, Contract no: HII3-CT-2003-505925. Financial support from the Netherlands Organisation for Scientific Research (NWO) for this work is gratefully acknowledged.

References

- [1] A.M. Glazer, Acta Crystallogr. B 28 (1972) 3384.
- [2] A.M. Glazer, Acta Crystallogr. A 31 (1975) 756.
- [3] C.J. Howard, H.T. Stokes, Acta Crystallogr. B 54 (1998) 782.
- [4] A. Putnis, Introduction to Mineral Sciences, Cambridge University Press, Cambridge, 1992.
- [5] B.J. Kennedy, C.J. Howard, Phys. Rev. B 59 (1999) 4023.
- [6] C.J. Howard, K.S. Knight, B.J. Kennedy, E. Kisi, J. Phys.: Condens. Matter 12 (2000) L677.
- [7] B.J. Kennedy, C.J. Howard, B.C. Chakoumakos, Phys. Rev. B 60 (1999) 2972.
- [8] B.J. Kennedy, B.A. Hunter, Phys. Rev. B 58 (1998) 653.
- [9] B.J. Kennedy, B.A. Hunter, J.R. Hester, Phys. Rev. B 65 (2002) 224103.
- [10] W.T. Fu, D. Visser, K.S. Knight, D.J.W. IJdo, J. Solid State Chem. 177 (2004) 1667.
- [11] K.S. Knight, Solid State Ion. 74 (1994) 109.
- [12] S.A. Ivanov, S.G. Eriksson, R. Tellgren, H. Rundlof, Mater. Sci. Forum 378–3 (2001) 511.
- [13] S.M. Moussa, B.J. Kennedy, T. Vogt, Solid State Comm. 119 (2001) 549.
- [14] J.R. Hester, C.J. Howard, B.J. Kennedy, R. Macquart, Aust. J. Chem. 55 (8) (2002) 543.
- [15] W.T. Fu, D. Visser, D.J.W. IJdo, Solid State Comm. 134 (2005) 647.
- [16] H. Ritter, J. Ihringer, J.K. Maichle, W. Prandl, A. Hoser, A.W. Hewat, Z. Phys. B 75 (1989) 297.
- [17] A.C. Larson, R.B. Von Dreele, GSAS General Structure Analysis System, Report LAUR 86-748. Los Alamos National Laboratory, Los Alamos, NM, 1986.
- [18] W.T. Fu et al., unpublished.
- [19] W.T. Fu, D.J.W. IJdo, J. Solid State Chem. 179 (2006) 2732.
- [20] A.D. Bruce, R.A. Cowley (Eds.), Structural Phase Transitions, Taylor & Francis, London, 1981.
- [21] M. Camprostrini, M. Hasenbusch, A. Pelissetto, P. Rossi, E. Vicari, Phys. Rev. B 65 (2002) 144520.
- [22] K.A. Müller, W. Berlinger, Phys. Rev. Lett. 26 (1971) 13.